

Generalising the staircase models

Patrick Dorey

Isaac Newton Institute for Mathematical Sciences,
20 Clarkson Road, Cambridge CB3 0EH, UK

and

CERN TH, 1211 Geneva 23, Switzerland
`dorey@surya11.cern.ch`

Francesco Ravanini

Isaac Newton Institute for Mathematical Sciences,
20 Clarkson Road, Cambridge CB3 0EH, UK

and

INFN – Sez. di Bologna,
Via Irnerio 46, I-40126 Bologna, Italy
`ravanini@bologna.infn.it`

Systems of integral equations are proposed which generalise those previously encountered in connection with the so-called staircase models. Under the assumption that these equations describe the finite-size effects of relativistic field theories via the Thermodynamic Bethe Ansatz, analytical and numerical evidence is given for the existence of a variety of new roaming renormalisation group trajectories. For each positive integer k and $s = 0, \dots, k-1$, there is a one-parameter family of trajectories, passing close by the coset conformal field theories $\mathcal{G}^{(k)} \times \mathcal{G}^{(nk+s)} / \mathcal{G}^{((n+1)k+s)}$ before finally flowing to a massive theory for $s=0$, or to another coset model for $s \neq 0$.

1. Introduction

The staircase model of Al. Zamolodchikov [1] is a simple relativistic factorized scattering theory in 1+1 dimensions, which shows signs of a very non-trivial renormalisation group behaviour. It describes a single boson with mass m and two-particle scattering amplitude

$$S(\theta) = \tanh\left(\frac{\theta - \theta_0}{2} - \frac{i\pi}{4}\right) \tanh\left(\frac{\theta + \theta_0}{2} - \frac{i\pi}{4}\right), \quad (1.1)$$

where θ_0 is a real parameter. Assuming the existence of an underlying field theory, the model can be studied at all length-scales by placing it on a cylinder and varying the circumference R . In particular, the ground-state scaling function $c(x)$ ($x = \log \frac{mR}{2}$) can be obtained by means of the Thermodynamic Bethe Ansatz (TBA) [2,3]. (The ground-state scaling function can be interpreted as an ‘effective central charge’ for the non scale-invariant theory, and is related to the vacuum Casimir energy by $E(R) = -\pi c(x)/6R$; for a unitary scale-invariant theory it is just equal to the central charge.) Plotting $c(x)$ as a function of x shows a series of plateaux, connected by steps each time x is near an integer or half-integer multiple of θ_0 . This staircase-like pattern becomes more pronounced as θ_0 increases, the values taken by $c(x)$ on the plateaux then running through the series $c_p = 1 - 6/p(p+1)$, the central charges of the $c < 1$ minimal models. This suggests an RG flow from an ultraviolet fixed point ($R \rightarrow 0$; $x \rightarrow -\infty$) with $c = 1$, to a trivial $c = 0$ fixed point in the infrared, passing close by each minimal model \mathcal{M}_p in turn. Varying θ_0 results in a one-parameter family of such flows; the larger θ_0 , the more closely the trajectory visits each minimal model in its journey from $c = 1$ to $c = 0$.

From another point of view, A. B. Zamolodchikov [4], and Ludwig and Cardy [5] showed some time ago that for large p the deformation of \mathcal{M}_p by its ϕ_{13} operator leads in the infrared to \mathcal{M}_{p-1} , so long as the coupling constant is positive. More recently, TBA analysis by Al. Zamolodchikov [6,7], applicable for all values of p , has reinforced this picture. The perturbed model, commonly denoted $\mathcal{M}A_p^{(+)}$, can thus be associated with an RG flow that hops between two neighbouring minimal models, and the staircase model can be seen as an approximation to this whole series of hopping flows, the approximation becoming better as θ_0 increases.

The minimal models are only the first of many infinite series of conformal field theories that can be constructed by means of the GKO coset construction [8]. For example, given any simple simply-laced Lie algebra $\mathcal{G} = A, D$ or E , there is a series of $W_{\mathcal{G}}$ -minimal models, rational conformal field theories described by the coset $\mathcal{G}^{(1)} \times \mathcal{G}^{(l)} / \mathcal{G}^{(1+l)}$. Since the minimal models are recovered by choosing $\mathcal{G} = A_1$, it is natural to ask whether staircase models can be found for the other $W_{\mathcal{G}}$ series. The fact that Zamolodchikov’s S-matrix

(1.1) is an analytic continuation in the coupling constant of the sinh-Gordon S-matrix (already remarked in ref. [1]) provides a strong hint that the required generalisation is to be found in the analytic continuation of the real-coupling affine Toda S-matrices, and this turns out to be the case [9,10]. To complete the analogy with the minimal sequence, it can be argued that ‘one-hop’ flows similar to those associated with the models $\mathcal{MA}_p^{(+)}$ should also exist for each $W_{\mathcal{G}}$ series. The generalisations of Zamolodchikov’s A_1 TBA analysis [6] to arbitrary \mathcal{G} [11,12] lend support to this view.

However this is by no means the end of the story. In particular, there are the models $\mathcal{G}^{(k)} \times \mathcal{G}^{(l)} / \mathcal{G}^{(k+l)}$ [13]. For each fixed k , they form a series with central charges $c_l = r(h+1)kl(k+2h+l)/(h+k)(h+l)(h+k+l)$, where r is the rank of \mathcal{G} and h the Coxeter number. In all cases, the operator analogous to ϕ_{13} is $\phi_{id,id,adj}$, the three indices labelling particular representations of $\mathcal{G}^{(k)}$, $\mathcal{G}^{(l)}$ and $\mathcal{G}^{(k+l)}$ respectively.

For $\mathcal{G} = A_1$, there are general perturbative results for large l matching those already described for the minimal models [14]. There is a surprise here, in that the perturbation of the l^{th} model of the k^{th} series does not flow to the $l-1^{\text{th}}$ model of this series, but rather to the $l-k^{\text{th}}$. As a result, there is no longer a single sequence of one-hop trajectories, but rather k disconnected sequences, interlaced along the k^{th} series. Note that taking $\mathcal{G} = A_1$, $k = 2$ gives the $N=1$ superconformal discrete series, for which this result had already been found in ref. [15]. A TBA analysis for the general A_1 case, for arbitrary values of l , has now been given by Al. Zamolodchikov [7]; the picture outlined above holds good modulo a small complication when l becomes smaller than k , which will be described later. The further generalisation to arbitrary \mathcal{G} can be found in ref. [12].

Since for given k there are k different sequences of hopping flows, it is reasonable to hope for k different staircase models approximating them. Some nice recent work by Martins [16,17] has started this programme by proposing a generalisation of Zamolodchikov’s original staircase model to one of the $k = 2$ sequences, finding TBA systems indicative of RG trajectories which pass close by the subset of superconformal minimal models with non-zero Witten index (l even), before flowing off to massive theories in the IR limit. He also showed the generalisation of this to other \mathcal{G} , again at $k = 2$ and l even. One interesting feature of his proposal is that each TBA system contains magnonic terms (pseudoenergies with no direct couplings to energy terms), perhaps indicating that the as-yet unknown scattering theories underlying the models have non-diagonal S-matrices.

In this paper, we propose and start to analyse TBA systems for general k and \mathcal{G} . The proposal itself is given in the next section: for each k there are k different systems, labelled by an index $s \in \mathbf{Z}_k$. In sections 3 and 4, we describe why these systems should mimic the desired hopping behaviour, a discussion that has many parallels to one given earlier for

the $k = 1$ series [10]. The conclusions of these two sections have been backed up by some numerical work, which is reported in section 5. The RG flows predicted have a number of surprising features, which can however be supported by alternative arguments. These points, along with some further speculations, are contained in the concluding section.

2. The spiral staircase

Take \mathcal{G} to be an arbitrary simply-laced Lie algebra, with Coxeter number h , and let a label nodes on the corresponding Dynkin diagram. In real-coupling affine Toda field theory, the different types of particle are labelled by just such an index; let m_a be the mass of the corresponding particle. These masses can also be characterised as the components of the Perron-Frobenius eigenvector of the \mathcal{G} Cartan matrix [18–20]. To provide for some magnonic structure, an extra label i will be needed, lying in \mathbf{Z}_k . As already mentioned, the particular staircase out of the k possibilities is determined by a member of \mathbf{Z}_k , s say, which will stay fixed throughout the discussion.

The TBA system will be given in terms of $r \times k$ pseudoenergies $\varepsilon_a^{(i)}$ (r is the rank of \mathcal{G}). The \mathbf{Z}_k -condition on the index i amounts to identifying $\varepsilon_a^{(i)}$ with $\varepsilon_a^{(i+k)}$. Similarly there are $r \times k$ energy terms $\nu_a^{(i)}$, given by the formula

$$\nu_a^{(i)}(\theta) = \widehat{m}_a(\delta^{i,0}e^{x-\theta} + \delta^{i,s}e^{x+\theta}), \quad (2.1)$$

where θ is the rapidity, and x encodes the scale of the system via $e^x = \frac{1}{2}m_1R$. The case $s=0$ will turn out to have a massive infrared limit, allowing m_1 to be interpreted as the mass of a particle, or multiplet of particles; the values of the remaining m_a are contained in the (dimensionless) ratios $\widehat{m}_a = m_a/m_1$. Note that the energy term is only nonzero if i is equal to 0 or s : it is in this way that the value of s enters the game. Defining $L_a^{(i)}(\theta) = \log(1 + e^{-\varepsilon_a^{(i)}(\theta)})$, and introducing a parameter $\theta_0 \in \mathbf{R}^+$, the proposed TBA system is:

$$\varepsilon_a^{(i)}(\theta) + \frac{1}{2\pi} \sum_{b=1}^r \left[\phi_{ab} * L_b^{(i)} - \psi_{ab} * L_b^{(i-1)}(\theta - \theta_0) - \psi_{ab} * L_b^{(i+1)}(\theta + \theta_0) \right] = \nu_a^{(i)}(\theta), \quad (2.2)$$

where all the i -type indices are to be taken modulo k , and $*$ denotes the rapidity convolution: $\phi * L(\theta) = \int_{-\infty}^{\infty} d\theta' \phi(\theta - \theta')L(\theta')$. The kernel functions ϕ_{ab} and ψ_{ab} are defined in terms of the minimal parts of the corresponding affine Toda S-matrix elements S_{ab}^{\min} , written in the form

$$S_{ab}^{\min}(\theta) = \prod_{x \in A_{ab}} (x-1)(\theta)(x+1)(\theta) \quad ; \quad (x)(\theta) = \frac{\sinh(\frac{\theta}{2} + \frac{i\pi x}{2h})}{\sinh(\frac{\theta}{2} - \frac{i\pi x}{2h})},$$

where A_{ab} is a set of integers (possibly with repetitions), and the related functions

$$S_{ab}^F(\theta) = \prod_{x \in A_{ab}} (x)(\theta).$$

Then

$$\phi_{ab}(\theta) = -i \frac{d}{d\theta} \log S^{\min}(\theta) \quad ; \quad \psi_{ab}(\theta) = -i \frac{d}{d\theta} \log S^F(\theta).$$

More explanation can be found in refs. [12,10]; while this notation is consistent with that of these two references, it differs from that of ref. [16]. A complete list of the functions S_{ab}^{\min} can be found in ref. [18], and general formulae in ref. [21].

The ground-state scaling function is now given in the standard way [3] in terms of the solutions to the TBA system (2.2), and the energy terms (2.1):

$$c(x, \theta_0) = \frac{6}{\pi^2} \sum_{a=1}^r \sum_{i=0}^{k-1} \int_{-\infty}^{\infty} d\theta \widehat{m}_a e^{x \nu_a^{(i)}(\theta)} L_a^{(i)}(\theta). \quad (2.3)$$

The next section will discuss the solutions to (2.2), explaining how the scaling function $c(x, \theta_0)$ can be expected to behave as a function of x . Before giving these details, it is worth making a few general comments on the system defined by (2.1) and (2.2). First, notice that just as in refs. [16,17], there are many ‘magnonic’ pseudoenergies with zero energy term: this may be a sign that for these models too, the underlying S-matrix is non-diagonal. More striking is the form that the shifted terms in (2.2) take: while the term shifted by $-\theta_0$ couples with $L_b^{(i-1)}$, that shifted by $+\theta_0$ couples with $L_b^{(i+1)}$. Thus these factors are not a simple continuation of the affine Toda Z-factors, as was the case for previous staircase TBA systems [1,9,10,16,17]. Despite the apparent asymmetry that this implies, the solutions of (2.2) are symmetric under $\theta \rightarrow -\theta$, so long as this transformation is accompanied by an exchange of the pseudoenergies $\varepsilon_a^{(i)} \rightarrow \varepsilon_a^{(s-i)}$. The possibility to implement the parity transformation in this way is a reflection of the symmetries of the affine \widehat{A}_k Dynkin diagram on which the \mathbf{Z}_k labels i live, and is reminiscent of the discussion for systems based on non-affine graphs given in ref. [22]. It also allows the ‘left-moving’ and ‘right-moving’ energy terms in (2.1) to be coupled to different pseudoenergies for $s \neq 0$, a hint that in these cases the system has a massless infrared limit. More detailed analysis in a later section will confirm this expectation.

The most important feature of (2.2) is the non-local nature of the interactions between the different pseudoenergies. The functions $\phi(\theta)$ and $\psi(\theta)$ are exponentially damped away from a region of order one about $\theta=0$, so their convolutions $\phi * L(\theta)$ and $\psi * L(\theta)$ are, up to exponentially small corrections, dominated by the values of $L(\theta')$ in a region of order

one about $\theta'=\theta$. (While functions $L(\theta)$ *could* be found for which this does not hold, suffice it to say that these do not seem to arise amongst the solutions to (2.2).) Hence the three convolution terms in (2.2), which involve $\varepsilon_a^{(i)}$, $\varepsilon_b^{(i-1)}$ and $\varepsilon_b^{(i+1)}$, pick up most of their values near θ , $\theta-\theta_0$, and $\theta+\theta_0$ respectively. To visualise this, it is helpful consider the index i on the same footing as θ , albeit only taking discrete values. Thus we write $\varepsilon_a^{(i)}(\theta) = \varepsilon_a(i, \theta)$, the pair (i, θ) being valued in $\mathbf{Z}_k \times \mathbf{R}$. This space has the form of a cylinder, on which (2.2) induces interactions between the neighbourhoods of (i, θ) , $(i-1, \theta-\theta_0)$ and $(i+1, \theta+\theta_0)$. This explains the sobriquet ‘spiral staircase’: the pseudoenergies couple together in a spiral pattern round the cylinder, a feature that turns out to be important in reproducing the expected hops in the RG flow.

3. The double helix

We now turn to the solutions to (2.2), and to progress we will have to make some more assumptions about their general form. These parallel the assumptions made in the analysis of more usual TBA systems, and we will not pretend to give any rigorous proofs. However, we have also made a number of numerical checks, which will be commented on later.

Comparing (2.2) and (2.1), there are two regions where $\varepsilon_a(i, \theta)$ and $L_a(i, \theta)$ are immediately known (as always, up to exponentially small corrections – we will tend to assume such a phrase to apply globally from now on). For $i = 0$ and $\theta \ll x$, the energy term $\nu_a(0, \theta)$ becomes very large and dominates (2.2), so that $\varepsilon_a(0, \theta \ll x) \approx \hat{m}_a e^{x-\theta}$. Correspondingly, $L_a(0, \theta \ll x)$ suffers a double-exponential decay and is soon negligably small. In the region $i = s$, $\theta \gg -x$, similar considerations show that $\varepsilon_a(s, \theta \gg -x)$ grows exponentially, while $L_a(s, \theta \gg -x)$ quickly decays towards zero.

Near to $(0, x)$, all the terms in (2.2) come into near-equal competition, and it is no longer a good approximation to ignore the convolutions. However, beyond this transitional region the form of the equation simplifies once again, as for $\theta \gg x$ the energy term $\nu_a(0, \theta)$ becomes exponentially small and can be dropped. On the basis of previously-studied TBA systems, we expect $L_a(0, \theta)$ to have a kink near $\theta = x$, interpolating between zero for $\theta \ll x$, and some other constant for $\theta \gg x$. Just as is the case for other TBA systems, the precise form of this kink is hard to find due to the increased complexity of (2.2) in the transitional region, but is not required for an asymptotic evaluation of the ground-state scaling function.

At this point the non-locality of (2.2) comes into play. The presence of a kink near $(0, x)$ has an effect, via the shifted convolution terms, on the equations obeyed near

$(k-1, x-\theta_0)$ and $(1, x+\theta_0)$. This is similar to the propagation of kinks in the $k=1$ staircase model described in [10], though with one important difference: here, the influence is on pseudoenergies with different values of i from that of the ‘seed’ kink near $(0, x)$, and hence with *different* energy terms derived from (2.1). In particular, while $L_a(0, \theta)$ was forced to be zero for $\theta \ll x$ by the dominance of $\nu_a(0, \theta)$ in this region, this is generally not the case for $L_a(k-1, \theta)$. Thus we expect to find kinks generated in *both* directions from the initial kink. These in turn cause there to be kinks at $(k-2, x-2\theta_0)$ and $(2, x+2\theta_0)$, and so on, the set of secondary kinks spiralling round the cylinder in both directions from $(0, x)$. Making the transformation $i \rightarrow s-i$, $\theta \rightarrow -\theta$ reveals another set of kinks spiraling away from $(s, -x)$, and interleaving with the first spiral to form the pattern of a double helix. This is illustrated in figure 1, where the kinks should be imagined to be strung out like beads along the two spirals. The two regions where the energy terms are dominant are depicted as double lines; the two seed kinks are at their ends. That they do not overlap means that the figure shows a situation where x is negative.

The asymptotic directions for which $c(x, \theta_0)$ can be evaluated correspond to the kinks from one spiral becoming far away from those of the other, so that the values of ε_a and L_a have time to settle down to approximately constant values in the inter-kink regions (that they *do* become nearly constant in these regions is in fact the key assumption of the discussion). This breaks down whenever $(m, x+n\theta_0) \approx (s, -x)$ for some m . The (strict!) equality implied on the \mathbf{Z}_k -valued first coordinate requires $m = nk+s$ for some integer n , and so interleaving will fail each time $x/\theta_0 \approx -(nk+s)/2$, corresponding to a crossover in the critical behaviour. Attention will now be restricted to situations far from these points, and the scaling function $c(x, \theta)$ treated in the limit $\theta_0 \rightarrow \infty$ with x/θ_0 remaining fixed at a value away from crossover.

While secondary kinks are generated in both directions from each seed kink, they cannot propagate indefinitely. The fact that \mathbf{Z}_k is cyclic means that at some stage energy terms will be re-encountered in domains where they are dominant, and this truncates the chain of kinks. For the remainder of this section, we assume that $x < 0$, as in figure 1; it will turn out that most (though not always all) of the hops are found in this region. For definiteness, take x to lie between crossovers in the region defined by

$$-(nk+s)\theta_0 \ll 2x \ll -((n-1)k+s)\theta_0. \quad (3.1)$$

Consider the spiral generated by the kink at $(0, x)$ (the behaviour of the other spiral will then follow by parity). After $k-1$ steps in the $-\theta$ -direction, there is a kink near $(1, x-(k-1)\theta_0)$. The energy term ν_a is zero in this region, and so there is no reason for this kink to be suppressed. However, one more step arrives at $(0, x-k\theta_0)$. This is well

inside the region $i = 0$, $\theta \ll x$ where, as already described, the part $\widehat{m}_a \delta^{i,0} e^{x-\theta}$ of the energy term dominates the TBA equation and forces $L_a(0, \theta)$ to be vanishingly small. There is no kink here – $L_a(0, \theta)$ has been zero since the seed kink at $(0, x)$, and remains so as θ decreases through $x - k\theta_0$. Thus in the $-\theta$ -direction, the chain of kinks terminates after $k-1$ steps. In the $+\theta$ direction, the truncation is instead effected by $\widehat{m}_a \delta^{i,s} e^{x+\theta}$, the part of the energy term which couples when $i = s$. If $\theta \ll -x$ this term plays no rôle in (2.2), and for x in the region (3.1) the spiral makes n complete circuits of the cylinder, and then continues with a further $s-1$ kinks, before the energy term becomes important. So, there are $nk+s-1$ kinks in the $+\theta$ -direction from the seed kink at $(0, x)$, truncation being caused by the suppression of the putative kink at $(s, x + (nk+s)\theta_0)$.

The full picture for both spirals can be seen by referring once again to figure 1: the spirals terminate when they encounter the double lines representing regions in which the energy term is completely dominant. Since they each make a single turn in one direction, and two complete turns in the other, the figure should correspond to taking $n=2$ in (3.1): this is easily verified by writing down the inequalities implied by the ordering of the marked points along the θ -axis.

We can now unwind each spiral from the cylinder, and represent the set of interacting kinks graphically:

$$\begin{array}{ccccccccc}
 & 1 & & k-1 & & k & & k+1 & & & & k+nk+s-1 \\
 \bigcirc & \text{---} & \text{---} & \bigcirc & \text{---} & \bigotimes & \text{---} & \bigcirc & \text{---} & \text{---} & \bigcirc & \text{---} & \bigcirc & \bigcirc
 \end{array} \tag{3.2}$$

Each node is a kink, and nodes are linked if they interact via the shifted convolution terms in (2.2). Empty nodes (\bigcirc) represent kink regions where the energy term plays no part in the leading behaviour of (2.2), while the filled node (\bigotimes) corresponds to the seed kink, in the neighbourhood of which the energy term $\widehat{m}_a \delta^{i,0} e^{x-\theta}$ cannot be ignored. This is also the only region of those represented on the graph which contributes directly to the formula (2.3) for $c(x, \theta_0)$. An isomorphic (reflected) graph results for the other spiral.

The next task is to find the values taken by the functions $\varepsilon_a(i, \theta)$ and $L_a(i, \theta)$ in the inter-kink regions. The necessary constraints follow in the usual way by pulling near-constant terms out of the convolutions in (2.2), leaving only overall integrals of ϕ_{ab} and ψ_{ab} . These are [19,12]:

$$\frac{1}{2\pi} \int_{-\infty}^{\infty} d\theta \phi_{ab}(\theta) = \delta_{ab} - 2C_{ab}^{-1} \quad ; \quad \frac{1}{2\pi} \int_{-\infty}^{\infty} d\theta \psi_{ab}(\theta) = -C_{ab}^{-1}, \tag{3.3}$$

where C_{ab} is the (non-affine) \mathcal{G} Cartan matrix. The various inter-kink regions influence each other through the non-local terms in (2.2), in much the same way as did the

kinks. To describe the situation, let the p^{th} kink in (3.2) be located near $(i_p, \theta_p) = (p \bmod k, x + (p-k)\theta_0)$, and let (i_p, θ_p^-) and (i_p, θ_p^+) be points in the inter-kink regions immediately before, respectively after, this kink:

$$\theta_p^- = \frac{1}{2}\theta_0(2p - (n+2)k - s) \quad ; \quad \theta_p^+ = \frac{1}{2}\theta_0(2p - (n+1)k - s). \quad (3.4)$$

Via (2.2), the $\varepsilon_a(i_p, \theta_p^-)$ come into interaction, as do the $\varepsilon_a(i_p, \theta_p^+)$. However care is needed when $p=k$. While the seed kink at $(i_k, \theta_k) = (0, x)$ owes its very existence to the delicate balance between the energy and convolution terms in (2.2) at that point, the energy term has become negligible by the time that (i_k, θ_k^+) is reached, and so has no effect on the equation for $\varepsilon_a(i_k, \theta_k^+)$. On the other hand, (i_k, θ_k^-) is in the region immediately to the left of the seed kink, where the energy term in (2.2) is dominant. As a consequence $\varepsilon_a(i_k, \theta_k^-)$ is forced to be effectively infinite, irrespective of the values taken by the other $\varepsilon_a(i_p, \theta_p^-)$.

All this has the effect of changing the ‘connectivity structure’ that for the kink interactions was summarised in (3.2). It can be visualised on figure 1 by mentally shifting the spiral based at $(0, x)$ slightly to the left, and then slightly to the right. Shifting leftwards, the spiral is cut by the double line representing a dominant energy term, while shifting rightwards disconnects the spiral from this line altogether, apart from the endpoint. Thus for the inter-kink regions containing the left-shifted points (i_p, θ_p^-) , (3.2) should be replaced by

$$\begin{array}{ccccccc} 1 & & k-1 & & k+1 & & k+nk+s-1 \\ \bigcirc & \text{---} & \bigcirc & & \bigcirc & \text{---} & \bigcirc \text{---} \bigcirc \end{array} \quad (3.5)$$

while to the right, the graph for the (i_p, θ_p^+) is

$$\begin{array}{ccccccc} 1 & & k-1 & k & k+1 & & k+nk+s-1 \\ \bigcirc & \text{---} & \bigcirc & \text{---} & \bigcirc & \text{---} & \bigcirc \text{---} \bigcirc \end{array} \quad (3.6)$$

For the second spiral making up the double helix, kinks are found at $(\tilde{i}_p, \tilde{\theta}_p) = (s - i_p, -\theta_p)$ and the two neighbouring inter-kink regions are centred on $(\tilde{i}_p, \tilde{\theta}_p^\pm)$, where $\tilde{\theta}_p^+ = -\theta_p^- = \theta_{(n+2)k+s-p}^-$ and $\tilde{\theta}_p^- = -\theta_p^+ = \theta_{(n+1)k+s-p}^-$. The above treatment goes through isomorphically when phrased in terms of these kinks, as indeed it must by the parity symmetry of the system.

To express the algebraic content of (3.5) and (3.6), let l_{pq}^- and l_{pq}^+ be their respective incidence matrices, and put $\tilde{C}_{pq}^\pm = 2\delta_{pq} - l_{pq}^\pm$. At (i_k, θ_k^-) , the value of ε_a has already been established; for the rest, extracting the near-constant values of $\varepsilon_a(i_p, \theta_p^\pm)$ from the

convolutions in (2.2) and using (3.3) yields, after some simple rearrangements, the following consistency conditions:

$$f_{ap}^{\pm} = \prod_{b=1}^r \prod_{q=1}^{(n+1)k+s-1} \left(1 - f_{bq}^{\pm}\right)^{C_{ab}^{-1} \tilde{C}_{pq}}, \quad (3.7)$$

where

$$f_{ap}^{\pm} = \frac{e^{-\varepsilon_a(i_p, \theta_p^{\pm})}}{1 + e^{-\varepsilon_a(i_p, \theta_p^{\pm})}}. \quad (3.8)$$

These equations reproduce the constraints for the limiting values of the pseudoenergies in the $\mathcal{G}^{(k)} \times \mathcal{G}^{(nk+s)} / \mathcal{G}^{((n+1)k+s)}$ TBA system given in [12], providing the substitution $\exp(-\varepsilon_a(i_p, \theta_p^{\pm})) = Y_p^a(\mp\infty)$ is made. While this is suggestive, caution is needed, since (3.7) describes the values of the functions ε_a at various points along the θ -axis, rather than just at $\pm\infty$ as for more usual systems. Nevertheless, asymptotically far from the crossovers the different kinks should become decoupled and behave like independent functions, their only interactions being those explicitly marked on (3.2). These reproduce exactly the interactions between different pseudoenergies found in the TBA systems of [7,12], so we certainly expect the evaluation of the function $c(x, \theta_0)$ in the asymptotic regime under discussion (given by (3.1)) to be the same as for the corresponding coset TBA system. But to confirm this, the leading asymptotic behaviour of $c(x, \theta_0)$ away from crossover can also be calculated directly from the formula (2.3), remaining within the spiral staircase model. The necessary modifications to the usual arguments have already been described at some length in ref. [10], and the slightly increased complexity of the models being considered here has no bearing on the calculations once the spirals have been unwound, and the connectivity structure (3.2) established. The one small point to watch is that since the massive kink is now located at the k^{th} position, inside the chain, the ‘integrations by parts’ by means of which the other kinks are felt now proceed in *both* directions away from k , rather than just to the right as for the $k=1$ staircase. Referring to the earlier paper [10] for further details, we will simply report the final result:

$$\lim_{\substack{\theta_0 \rightarrow \infty \\ x/\theta_0 = N_n}} c(x, \theta_0) = c_n = \frac{6}{\pi^2} \sum_{a=1}^r \sum_{q=1}^{(n+1)k+s-1} [\mathcal{L}(f_{ap}^+) - \mathcal{L}(f_{ap}^-)], \quad (3.9)$$

where x/θ_0 is held fixed at N_n , $-(nk+s)/2 \ll N_n \ll -((n-1)k+s)/2$, while the limit is taken in order to stay inside the regime defined by (3.1). The functions appearing on the righthand side are Rogers dilogarithms, defined by $\mathcal{L}(z) = -\frac{1}{2} \int_0^z dt \left(\frac{\log(1-t)}{t} + \frac{\log t}{1-t} \right)$, and their arguments f_{ap}^{\pm} are obtained by solving (3.7). To finish the calculation, a sum rule

is needed [23]: if $\{f_{ap}\}$ ($1 \leq a \leq r$, $1 \leq p \leq l$) is the solution to (3.7) when C_{ab} is the Cartan matrix of \mathcal{G} and \tilde{C}_{pq} the Cartan matrix of the algebra $A_{r'}$, then

$$\frac{6}{\pi^2} \sum_{a=1}^r \sum_{p=1}^{r'} \mathcal{L}(f_{ap}) = \frac{rr'h'}{h+h'} = rh' - \frac{r(h+1)h'}{h+h'}, \quad (3.10)$$

where h is the Coxeter number of \mathcal{G} and $h'=r'+1$ the Coxeter number of $A_{r'}$. The second version is useful because it shows the sum to be rh' minus the central charge of the $\mathcal{G}^{(h')}$ WZW model. For the case in hand, the sum over the $\mathcal{L}(f_{ap}^+)$ follows from (3.10) with $h' = (n+1)k+s$, since (3.6) is the Dynkin diagram of $A_{(n+1)k+s-1}$. For the $\{f_{ap}^-\}$ there are two disconnected parts to (3.5), the Dynkin diagrams of A_{k-1} and A_{nk+s-1} . Correspondingly the dilogarithm sum splits into two, summed by taking h' equal to k and $nk+s$ respectively. The absent k^{th} node does not contribute since $\mathcal{L}(f_{ak}^-) = \mathcal{L}(0) = 0$ for all a , and so

$$c_n = r(h+1) \left[\frac{k}{h+k} + \frac{nk+s}{h+nk+s} - \frac{(n+1)k+s}{h+(n+1)k+s} \right], \quad (3.11)$$

the central charge of the $\mathcal{G}^{(k)} \times \mathcal{G}^{(nk+s)} / \mathcal{G}^{((n+1)k+s)}$ coset model.

4. The infrared limit

To complete the picture of the asymptotics of the ground-state scaling function $c(x, \theta_0)$, the condition that x be negative, imposed throughout the last section, must be relaxed. Since x is related to the physical parameters of the model by $\frac{1}{2}m_1 R = e^x$, this corresponds to examining the system in the infrared.

The point to note is that for x positive the nature of the relationship between the spirals of kinks and the two regions of energy-term dominance, illustrated in figure 1 for x negative, may change. When x becomes positive, the two regions, marked by double lines on figure 1, start to overlap, as in one region θ runs from $-\infty$ to x , in the other from $-x$ to $+\infty$. If $s = 0$, then the two regions actually collide and this has the effect of killing off the two seed kinks completely. Thus in this case the IR limit is simple: a theory with $c = 0$, with the final crossover to a massive phase occurring near $x = 0$. Otherwise, kinks will continue to be found near $(0, x)$ and $(s, -x)$ for arbitrarily large positive values of x . Thus the $L_a^{(i)}(\theta)$ never become trivial, and a non-zero value for $c(x, \theta_0)$ is expected even as $x \rightarrow +\infty$. This reinforces the assertion made in section 2 that for $s \neq 0$ the IR limit of (2.2) should be massless. Precisely which conformal field theory this massless limit should be brings one last surprise. In the previous discussion it was seen that for $x < 0$ the spiral generated at $(0, x)$ truncates after a single turn in the $-\theta$ direction, when it re-encounters

the $i=0$ energy term. This is why the left-most piece of (3.5) has $k-1$ nodes, and one of the elements of the coset whose central charge (3.9) reproduces has level k . But if x is positive, this can change. In the $-\theta$ direction, the chain from $(0, x)$ might encounter the energy term at $i=s$ *before* returning to $i=0$. The onset of this phenomenon is signalled by a crossover around $x = \frac{1}{2}(k-s)\theta_0$, beyond which point the chain of kinks anchored at $(x, 0)$ is terminated in *both* directions by the $i=s$ energy term. It is straightforwardly seen that this is the last such crossover expected on the basis of changes to the overall kink structure, and that after this point the situation stabilises, the form of the pseudoenergies remaining unchanged apart from simple translations as $x \rightarrow +\infty$. The final kink system, governing the IR limit, can be unwound and represented graphically just as before. The picture (3.2) becomes:

$$\begin{array}{cccccc} s+1 & & k-1 & & k & & k+1 & k+s-1 \\ \circ & - & \circ & - & \otimes & - & \circ & - & \circ \end{array} \quad (4.1)$$

where to ease comparison with the earlier graphs, the mod- k values of the labels have been preserved. This graph has $k-s-1$ massless nodes to the left, $s-1$ to the right. The remaining calculations now go through unchanged, (3.9) becoming

$$\lim_{\substack{\theta_0 \rightarrow \infty \\ x/\theta_0 = N_{-1} \gg (k-s)/2}} c(x, \theta_0) = c_{-1} = r(h+1) \left[\frac{k-s}{h+k-s} + \frac{s}{h+s} - \frac{k}{h+k} \right], \quad (4.2)$$

which is the central charge of the $\mathcal{G}^{(k-s)} \times \mathcal{G}^{(s)} / \mathcal{G}^{(k)}$ coset model.

In this last equation, the fact that N_{-1} is positive means that x tends to $+\infty$ as the limit $\theta_0 \rightarrow \infty$ is taken, but this does not spoil the validity of the asymptotic estimates being made. However, the real interest all along has been to trace the variation in $c(x, \theta_0)$ in one particular model, for which θ_0 is fixed. Thus a change in the point of view is needed to apply the results found so far. If the value of θ_0 is large enough, then as x varies, the pair (x, θ_0) will pass through a series of regions for which the asymptotic results (3.9) and (4.2) are good approximations to the true values of $c(x, \theta_0)$. Hence this function will run through the values c_n in turn, deviating significantly from these numbers only in the crossover regions. An order-of-magnitude estimate for the size of these regions is easily given: the approximations leading up to (3.9) and (4.2) were good, up to exponentially small corrections, so long as the various kinks in each pseudoenergy $\varepsilon_a^{(i)}(\theta)$ were clearly separated along the θ -axis. These kinks have a size of order one (the precise value will depend on the model, but in any case we are only interested in orders of magnitude in comparison with x and θ_0 here), and so the crossover will start when the expected

positions of two kinks become closer than this. There are generally two different interkink separations for any given (x, θ_0) (this is rather clear from looking at figure 1); they are:

$$\begin{aligned}\theta_p - \tilde{\theta}_{(n+1)k+s-p} &= -2x - ((n-1)k + s)\theta_0; \\ \tilde{\theta}_{(n+1)k+s-p} - \theta_{p+k} &= 2x + (nk + s)\theta_0.\end{aligned}\tag{4.3}$$

(That these two are positive follows from (3.1); strictly speaking there are also steadily growing separations for x larger than the final crossover, after the two spirals have become completely disentangled.) The interkink separations are therefore overly small only in regions of order one about each crossover value of x . Since the intervals between these crossover values grow linearly with θ_0 , the staircase-like nature of $c(x, \theta_0)$ soon becomes pronounced. This is the evidence for the previously-advertised roaming RG trajectories, and from the values of c_n , the set of fixed points approached by any particular flow can be read off. The $\mathcal{G}^{(k)} \times \mathcal{G}^{(l)} / \mathcal{G}^{(k+l)}$ coset models can be imagined to be located on a grid, giving the following skeleton for the large- θ_0 pattern of the k, s ($s \neq 0$) flow:

$$\begin{aligned}& \downarrow \\ & c(k, 2k + s) \\ & \downarrow \\ & c(k, k + s) \\ & \downarrow \\ & c(k - s, s) \leftarrow c(k, s)\end{aligned}\tag{4.4}$$

The set-up for $s=0$ is less unexpected:

$$\begin{aligned}& \downarrow \\ & c(k, 2k) \\ & \downarrow \\ & c(k, k) \\ & \downarrow \\ & 0 \text{ (massive)}\end{aligned}\tag{4.5}$$

Before attempting to interpret these results, it is worth seeing that they stand up to numerical verification.

5. Numerical work

The above has relied rather heavily on assumptions about the behaviour of the solutions to (2.2) – the existence of kinks and so on – which, though well-motivated, have most certainly not been rigorously derived. Therefore it is worth subjecting the proposal to some independent checks, and for this we have solved the equations (2.2) numerically in a number of cases, discretising the θ axis at intervals of 0.2, and then iterating (2.2) until $c(x, \theta_0)$ relaxed to a steady value. To gain five-digit precision, ample for the purposes of graph-plotting, typically took from 25 to 30 steps. We have only looked at the case $\mathcal{G} = A_1$ – for higher-rank algebras the iteration of TBA equations, even in the usual cases, is more tricky [24] – but previous numerical work on higher-rank staircase models [9,16,17] gives no reason to expect any unpleasant surprises. In particular, in refs. [16,17] Martins proposed and investigated numerically the $k = 2, s = 0$ instance of (2.2) with $\mathcal{G} = A_2$, and the predictions made above for this case are consistent with his findings.

Figures 2a and 2b show numerical results for all values of s at $k = 2$ and $k = 3$, respectively. In both cases θ_0 was fixed at 40, and it can be seen that the agreement with the predictions of the last two sections is excellent, even including the final ‘corner’ of (4.4) for $s \neq 0$. One amusing feature is that for $k = 3$, the two flows with non-zero s have the same infra-red central charge, despite their very different behaviours at intermediate scales. At given k , each pair of flows $s, k-s$ has this property – at the simplest level just a reflection of the fact that $c(\mathcal{G}^{(k-s)} \times \mathcal{G}^{(s)} / \mathcal{G}^{(k)}) = c(\mathcal{G}^{(s)} \times \mathcal{G}^{(k-s)} / \mathcal{G}^{(k)})$. Note though that this is only an equality of central charges – since our system in its current form only traces the evolution of the ground-state energy, we cannot distinguish between different modular invariants having the same central charge.

6. Discussion

The convergence of analytical and numerical results leaves little doubt that the behaviour of the solutions to (2.2) is as claimed above, even if this has not been rigorously proved. It is then very tempting to suppose that (2.2) is indeed the TBA system for some relativistic field theory, the exact ground-state scaling function of which is given by $c(x, \theta_0)$. In the absence of any concrete proposals as to what this model might be, we can at least discuss some of its expected properties, and decide whether they are consistent from other points of view.

The first of these properties is that as x increases from the deep ultraviolet, $c(x, \theta_0)$ does indeed run through the sequence of numbers c_n given by equation (3.11), these being a subset of the $\mathcal{G}^{(k)} \times \mathcal{G}^{(l)} / \mathcal{G}^{(k+l)}$ central charges. The function pauses near each c_n for a

‘time’ approximately given by $k\theta_0/2$ for large θ_0 , before making a sharp transition to c_{n-1} over an interval with size of order one, in the process of which l decreases by k . This is just the behaviour needed for a staircase model based on these cosets, being consistent with the existence of a family of roaming flows which in the large- θ_0 limit comes to approximate the known single-hop trajectories.

More interesting is the predicted behaviour towards the infrared, as x increases and l becomes smaller. The hopping-by- k cannot continue indefinitely, since l cannot be negative. For $s=0$, the situation is simple: after a last pause near $l=k$, the final flow is to $c=0$, implying that the theory becomes massive at long distances. All previously-studied staircase models have shared this property, which is furthermore in accord with the one-hop behaviour predicted for the $\phi_{id,id,adj}$ -perturbation of a $\mathcal{G}^{(k)} \times \mathcal{G}^{(k)} / \mathcal{G}^{(2k)}$ coset model. To understand the curious final hop that all the staircase systems with $s \neq 0$ undergo, we first recall the general small- l pattern of the interpolating trajectories [7]. Even without the TBA, it is clear that once l has become smaller than k , it is no longer possible for l to decrease by a further k . However the perturbation $\phi_{id,id,adj}$ is symmetrical with respect to the k and l in the numerator of the coset $\mathcal{G}^{(k)} \times \mathcal{G}^{(l)} / \mathcal{G}^{(k+l)}$, and so as soon as l decreases below k , it is natural to expect that the flow induced by this perturbation now hops by decreasing k by an amount l , instead of l by k . Such a change in direction for the interpolating trajectories when l becomes smaller than k is indeed predicted by Zamolodchikov’s TBA analysis [7].

For the superconformal discrete series ($\mathcal{G}=A_1$ and $k=2$), such a phenomenon was discussed in ref. [25], and can be visualised by referring back to figure 2a, which shows the form of the two flows predicted by (2.2) for this case. The series of models with l odd continues to hop down in steps of 2 until $l=1$, the tricritical Ising model, is reached. All of the models up to and including this point have been $N=1$ supersymmetric, a symmetry respected by their $\phi_{id,id,adj}$ perturbations – the field is in fact the top component of a supermultiplet, all other components vanishing anyway on integration over the Grassman directions. However while the $\phi_{id,id,adj}$ operator of the tricritical Ising model again respects the $N=1$ supersymmetry, it is also the ϕ_{13} operator in the sense of the minimal $c<1$ series, and as such induces a flow down to the Ising model, which does *not* possess such a symmetry. The interpretation given in ref. [25] is that the supersymmetry is spontaneously broken along this last trajectory. At large θ_0 we can expect the $k=2, s=1$ staircase model to show similar behaviour, with an approximate supersymmetry at short distances being broken near $x=\theta_0/2$ as the trajectory approximates the final step down to the Ising model. Thus a change in the hop direction, from decreasing l to decreasing k , is not ruled out, and should probably be associated with the spontaneous breaking of whatever higher

symmetry is associated with a given series. For $k=2$, this was $N=1$ supersymmetry, and the situation was reasonably under control; for large values of k , or algebras \mathcal{G} other than A_1 , the situation is less clear, and the discussion much more speculative. The possible forms of the symmetries associated with such theories were first discussed in refs. [26], and later in ref. [27] where they were called ‘fractional supersymmetries’, but in particular the lack of a satisfactory generalisation of the Grassman variables to these situations makes life difficult. A better understanding of all this will be needed before any detailed implications can be drawn for the symmetries of the staircase models.

To return to the general form of the staircase flows, it is tempting to imagine that they should ultimately approximate a complete sequence of these single hops, joined up nose-to-tail to form a zig-zag series of flows with the left and right coset indices taking turns to decrease, until a diagonal coset ($k=l$) is reached, at which point the flow would be to a massive model. However this is *not* what happens for the spiral staircase flows predicted by (2.2) and illustrated in (4.4): after only a single hop in a new direction, the flow grinds to a halt, the final destination in the infrared being the $\mathcal{G}^{(k-s)} \times \mathcal{G}^{(s)} / \mathcal{G}^{(k)}$ coset. In terms of the higher symmetries touched on above, the staircase continues to mimic the sequence of single-hop flows only so long as the perturbing operator respects the symmetry associated with the k^{th} series of cosets – after the final flow in which the symmetry is spontaneously broken, there are no longer any directions respecting this symmetry, and the flow is ‘trapped’.

For an alternative understanding of why the flow might come to such an abrupt stop, first recall some work by Lässig [28] on Zamolodchikov’s original staircase model. The hopping flows mimicked in this case were those between minimal models, $\mathcal{M}_p \rightarrow \mathcal{M}_{p-1}$, induced by the massless ϕ_{13} perturbation. Lässig pointed out that at large p an RG flow with properties identical to that predicted by Zamolodchikov can be uncovered within a perturbative treatment, simply by adding the slightly irrelevant operator ϕ_{31} to the original perturbation by the just-relevant operator ϕ_{13} . Normally one ignores irrelevant operators as having no effect on the infrared destination of an RG trajectory, but this may not be correct if the situation under discussion involves a crossover in critical behaviour, as here. The subtlety is that even an irrelevant operator with respect to the first fixed point may induce couplings to relevant operators near the second, repelling the trajectory and sending it on to some new destination of even lower criticality. A detailed analysis of the relevant RG equations, to lowest order in $1/p$, shows that this is indeed what happens for the combined ϕ_{13}, ϕ_{31} flows in the minimal series – in fact, both operators are nearly marginal and mix under the RG flow, so that, crudely speaking, the irrelevant ϕ_{31} operator near \mathcal{M}_p becomes ϕ_{13} as \mathcal{M}_{p-1} is approached, and sends the flow leapfrogging on down

the minimal sequence. Thus even an irrelevant operator can cause an interpolating flow to change its IR behaviour, a judicious choice managing to replicate itself at the next step, and ultimately producing a flow with the characteristic staircase-like form. It is important here that the original perturbing operator for the interpolating flow, ϕ_{13} , flowed precisely to ϕ_{31} in the infrared – had it flowed to anything else, the subspace of couplings under consideration would have had to be enlarged at least to include that operator, spoiling the simple leapfrogging picture. To repeat this analysis for a level- k staircase, it is therefore natural to imagine a $\mathcal{G}^{(k)} \times \mathcal{G}^{(l)} / \mathcal{G}^{(k+l)}$ model perturbed by a linear combination of the relevant operator $\phi_{UV}^{(k,l)} = \phi_{id,adj,id}$, which on its own induces the interpolating flow to the next model down, and the irrelevant operator $\phi_{IR}^{(k,l+k)}$, along which the trajectory arriving from the model one step higher arrives. (There is also an incoming flow $\phi_{IR}^{(k+l,l)}$ forming part of a level- l sequence of hops, but we won't worry about this for now.) In ref. [7], Zamolodchikov found the incoming operator in the case $\mathcal{G} = A_1$ to have conformal dimension

$$\Delta_{IR} = 1 + \frac{2}{l+2}, \quad (6.1)$$

corresponding to the field $\phi_{id,adj,id}$. The flow into $l=1$ is exceptional, in that there is no operator in the infrared model with this conformal dimension – the adjoint is not among the level-one representations of $\widehat{SU}(2)$. Instead, the prediction is that $\Delta_{IR}=2$, leading to the expectation that here the attracting operator is $T\bar{T}$. Staying with this case, which for the spiral staircase corresponds to setting $s=1$, we should examine the effect of adding some $T\bar{T}$ to the ϕ_{13} -perturbation of the $(k, 1)$ A_1 coset model. For large k a treatment perturbative in $1/k$ should be valid. Note that even in this limit the operator $T\bar{T}$ retains a scaling dimension of 4, a feature which already distinguishes this case from that of the combined ϕ_{13}, ϕ_{31} perturbations. But more important is the fact that $T\bar{T}$ is a symmetrical descendant of the identity, so that the operators generated in repeated operator product expansions of ϕ_{13} and $T\bar{T}$ only consist of left-right symmetric descendants of ϕ_{13} . Since ϕ_{13} itself is already nearly marginal in the large- k limit, any such descendants will be strongly irrelevant. Any operator mixing induced through the RG flow is restricted to operators in this subalgebra, and therefore should not affect the final destination of the flow. Near to the $(k, 1)$ fixed point (\mathcal{M}_{k+2}), there are thus (at least) two different subspaces pertinent to staircases: one spanned by ϕ_{13} and ϕ_{31} , and one by ϕ_{13} and $T\bar{T}$. The first of these is relevant to the original ($k=1$) staircase of Zamolodchikov, as shown by Lässig, while we expect the second to contain the tail-end of the k^{th} A_1 spiral staircase model at $s=1$, undergoing its final crossover before flowing down to the coset model at $(k-1, 1)$ in the far infrared. The more detailed analysis made by Lässig also gave signs of other flows complementary to the staircase, obtained by varying the signs of the couplings. It would

be interesting to investigate these possibilities, but for the moment we content ourselves with this plausibility argument for the form of the final step of the $s=1$ spiral staircase.

There do not appear to be any obstructions in principle to applying analogous arguments in the cases $s>1$ and/or $\mathcal{G}\neq A_1$. Zamolodchikov [7] found that in the case relevant for our $\mathcal{G} = A_1$, $s=2$ staircases, the incoming direction at the end of the second-last crossover mimicked by the roaming flow is $G\bar{G}$, rather than the $T\bar{T}$ above, where G is the spin $3/2$ part of the supercurrent. This is certainly suggestive, but to give a satisfactory analysis of the general case requires a more detailed knowledge of the fractional supersymmetry algebras than we have at present.

A final area for further speculation concerns the field theories underlying our TBA systems. If such models exist, they must have a rich and varied structure, and only a subset of them can be massive. On the basis of the magnonic structure, we would expect to find non-diagonal scattering in these cases. The $k=1$ systems were intimately related to the real-coupling affine Toda theories [9,10], and so it is possible that further insight may be found in the fractional supersymmetric sine-Gordon models introduced by Bernard and LeClair [27]. While we have no definite suggestions to make in this direction, it seems to be an interesting area for further work.

Acknowledgements

We would like to thank the Isaac Newton Institute for its hospitality during the completion of this work, and John Cardy for useful discussions. PED thanks Márcio Martins for sending a copy of his paper [16] prior to publication. This work was supported by a grant under the EC Science Programme (PED), and by the Isaac Newton Institute and INFN (FR), all of whom we acknowledge and thank.

References

- [1] Al. B. Zamolodchikov, “Resonance factorized scattering and roaming trajectories”, preprint ENS-LPS-335, 1991.
- [2] C. N. Yang and C. P. Yang, *J. Math. Phys.* **10** (1969) 1115.
- [3] Al. B. Zamolodchikov, “Thermodynamic Bethe Ansatz in Relativistic Models. Scaling 3-state Potts and Lee-Yang Models”, *Nucl. Phys.* **B242** (1990) 695.
- [4] A. B. Zamolodchikov, “Renormalization group and perturbation theory about fixed points in two-dimensional field theory”, *Sov. J. Nucl. Phys.* **46** (1987) 1090.
- [5] A. W. W. Ludwig and J. L. Cardy, “Perturbative evaluation of the conformal anomaly at new critical points with applications to random systems”, *Nucl. Phys.* **B285** (1987) 687.
- [6] Al. B. Zamolodchikov, “Thermodynamic Bethe Ansatz for RSOS scattering theories”, *Nucl. Phys.* **B358** (1991) 497;
Al. B. Zamolodchikov, “From tricritical Ising to critical Ising by Thermodynamic Bethe Ansatz”, *Nucl. Phys.* **B358** (1991) 524.
- [7] Al. B. Zamolodchikov, “TBA equations for integrable perturbed $SU(2)_k \times SU(2)_l / SU(2)_{k+l}$ coset models”, *Nucl. Phys.* **B366** (1991) 122.
- [8] P. Goddard, A. Kent and D. Olive, *Phys. Lett.* **B152** (1985) 88; *Comm. Math. Phys.* **103** (1986) 105.
- [9] M. J. Martins, “Renormalization group trajectories from resonance factorized S-matrices”, preprint SISSA-EP-72, *Phys. Rev. Lett.* in press;
M. J. Martins, “Exact resonance A-D-E S-matrices and their renormalization group trajectories”, preprint SISSA-EP-85.
- [10] P. E. Dorey and F. Ravanini, “Staircase models from affine Toda field theory”, preprint SPhT/92-065, DFUB-92-09, *Int. J. Mod. Phys. A* in press.
- [11] M. J. Martins, “The Thermodynamic Bethe Ansatz for deformed WA_{N-1} conformal field theories”, *Phys. Lett.* **B277** (1992) 301.
- [12] F. Ravanini, “Thermodynamic Bethe Ansatz for $\mathcal{G}_k \otimes \mathcal{G}_l / \mathcal{G}_{k+l}$ coset models perturbed by their $\phi_{1,1,Adj}$ operator”, *Phys. Lett.* **B282** (1992) 73.
- [13] P. Christe and F. Ravanini, “ $G_N \otimes G_L / G_{N+L}$ conformal field theories and their modular invariant partition functions”, *Int. J. Mod. Phys. A* **4** (1989) 897.
- [14] C. Crnković, G. M. Sotkov and M. Stanishkov, “Renormalization group flow for general $SU(2)$ coset models”, *Phys. Lett.* **B226** (1989) 297.
- [15] R. G. Pogosyan, “Study of the neighbourhoods of superconformal fixed points in two-dimensional field theory”, *Sov. J. Nucl. Phys.* **48** (1988) 763;
Y. Kitazawa, N. Ishibashi, A. Kato, K. Kobayashi, Y. Matsuo and S. Odake, “Operators product expansion coefficients in $N = 1$ superconformal theory and slightly relevant perturbation”, *Nucl. Phys.* **B306** (1988) 425.

- [16] M. J. Martins, “Analysis of asymptotic conditions in resonance functional hierarchies”, preprint SISSA-EP-151.
- [17] M. J. Martins, “RG flows and resonance scattering amplitudes”, preprint SISSA-EP-154.
- [18] H. W. Braden, E. Corrigan, P. E. Dorey and R. Sasaki, “Affine Toda field theory and exact S-matrices”, *Nucl. Phys.* **B338** (1990) 689.
- [19] T. R. Klassen and E. Melzer, “Purely elastic scattering theories and their ultraviolet limits”, *Nucl. Phys.* **B338** (1990) 485.
- [20] M. D. Freeman, “On the mass spectrum of affine Toda field theory”, *Phys. Lett.* **B261** (1991) 57.
- [21] P. E. Dorey, *Nucl. Phys.* **B358** (1991) 654; *Nucl. Phys.* **B374** (1992) 741.
- [22] F. Ravanini, R. Tateo and A. Valleriani, “Dynkin TBAs”, preprint DFUB-92-11, DFTT-31/92.
- [23] A. N. Kirillov, *Zapiski Nauch. Semin. LOMI* **164** (1987) 121;
V. V. Bazhanov and N. Reshetikhin, *J. Phys.* **A23** (1990) 1477.
- [24] T. R. Klassen and E. Melzer, “The thermodynamics of purely elastic scattering theories and conformal perturbation theory”, *Nucl. Phys.* **B350** (1991) 635.
- [25] D. Kastor, E. Martinec and S. Shenker, “RG flow in $N = 1$ discrete series”, *Nucl. Phys.* **B316** (1989) 590.
- [26] F. Ravanini, “An infinite class of new conformal field theories with extended algebras”, *Mod. Phys. Lett.* **A3** (1988) 397;
J. Bagger, D. Nemeschansky and S. Yankielowicz, “Virasoro algebras with central charge $c > 1$ ”, *Phys. Rev. Lett.* **60** (1988) 389;
D. Kastor, E. Martinec and Z. Qiu, “Current algebra and conformal discrete series”, *Phys. Lett.* **B200** (1988) 434.
- [27] D. Bernard and A. LeClair, “The fractional supersymmetric sine-Gordon models”, *Phys. Lett.* **B247** (1990) 309.
- [28] M. Lässig, “Multiple crossover phenomena and scale hopping in two dimensions”, *Nucl. Phys.* **B380** (1992) 601;
M. Lässig, “Exact critical exponents of the staircase model”, Jülich preprint (February 1992).

Figure 1 : The arrangement of kinks around the cylinder.

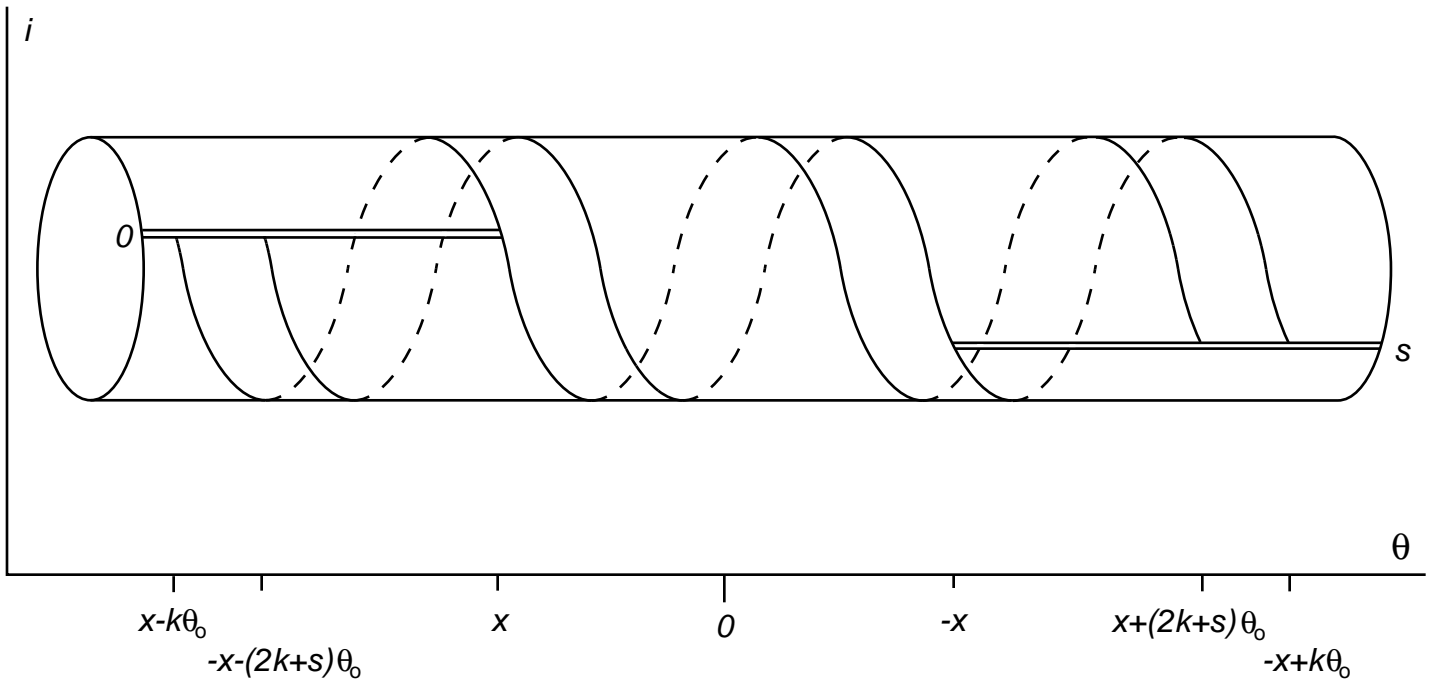


Figure 2 : Plots of ground state scaling functions.

